Comet Bowell at record heliocentric distance

Karen J. Meech & David Jewitt

Department of Earth, Atmospheric and Planetary Sciences, Massachusetts Institute of Technology, Cambridge, Massachusetts 02139, USA

Comets probably contain the most primordial material in the Solar System, and those which are passing through the inner Solar System for the first time are likely to be the most pristine of all. Comet Bowell (1982 $I = 1980b$) was discovered in 1980 at the unusually large heliocentric distance of $R = 7.3$ AU (ref. 1). The small reciprocal of the original orbital semi-major axis, $(1/a) = 30 \times 10^{-6}$ AU^{-1}, suggests that this comet is dynamically new in the sense that it has made few, if any, previous passages through the inner Solar System[2]. Because prolonged solar irradiation may alter the properties of short-period comets, it is of great interest to see if 1982 I exhibits properties which are significantly different from those of the periodic comets. We present new observations of comet Bowell at the record distance $R = 13.6$ AU. An extended coma is present, the size of which is consistent with the same slow expansion rate $v \approx 1$ m s^{-1} detected around perihelion (March 1982 and $R \approx 3.36$ AU). The cross-section of the solid grains within the central 10 arc s of the coma has decreased by over an order of magnitude since 1980–1984, which indicates that the coma production is declining. The decline began near $R \approx 10$ AU, the same distance at which production began on the pre-perihelion leg. The coma at $R \leq 10$ AU may be formed by sublimation of CO_2 or an ice of similar volatility from the nucleus.

We briefly summarize the major characteristics of 1982 I previously determined from observations around perihelion (1980–84). The comet is known to exhibit substantial activity at distances beyond which H_2O sublimation is expected to be significant ($R \geq 6$ AU). Its lightcurve is quite different from that of comet Halley, in which the activity is controlled largely by H_2O sublimation[3]. There has been one reported detection of H_2O ice in the near infrared spectrum of this comet[4], however the identification is controversial[5]. Other near infrared spectra of the comet show no evidence for H_2O ice[5,6], and water-ice sublimation models are unable to reproduce the lightcurve[7]. More volatile ices, typified by N_2, provide a better (but not perfect) match to the near-perihelion photometry[7]. The best match to the photometry is provided by an inert coma, but the solid-grain coma was found to expand at a very low velocity $v = 0.9 \pm 0.2$ m s^{-1} (refs 7, 8). Estimates of the ratio of the radiation pressure acceleration to the gravitational acceleration of particles in the tail indicate that comet Bowell has an unusual particle size distribution, with a deficiency of particles of radii $a \leq 300$–400 μm (ref. 8). Given the unusual properties of the comet and the likelihood that H_2O sublimation was not responsible for its activity at $R \geq 6$ AU, we were encouraged to attempt to observe this comet at extremely large R to obtain information about the physical processes controlling the activity on the nucleus.

The present observations were obtained with the Kitt Peak 2.1-m telescope and an 800 × 800 Texas Instruments charge-coupled device (CCD), using an ephemeris provided by B. G. Marsden (personal communication). Four images of 900 s each were taken through a Mould R filter on 3 November 1986 UT ($R = 13.6$ AU), with the telescope tracked at sidereal rate (see Table 1 for observational parameters). The comet appeared as a diffuse patch of extremely low surface brightness which clearly showed the expected motion between exposures. A summed image of comet Bowell, made by shifting the individual images according to the ephemeris motion (giving an effective exposure of 1 hour), is shown in Fig. 1*a*. A line diagram of the same image showing the location of the comet with respect to trailed stars is given in Fig. 1*b*. Unmarked diffuse features in Fig. 1*a* are faint field galaxies. We also detected comet Bowell (at $R = 11.0$ AU) on 21 September 1986 UT (see Table 1) using the Kitt Peak 4-m telescope with the same CCD at the prime focus.

The brightness profile of the comet at $R = 13.6$ AU is shown in Fig. 2. The brightness was measured as a function of projected distance from the nucleus along a line drawn perpendicular to the projected orbit. From Fig. 2 we obtain an estimate of the lower limit of the radius of the coma as $P_{13.6\,\mathrm{AU}} = 15 \pm 2$ arc s. A similar measurement from the 4-m image yields $P_{11.0\,\mathrm{AU}} = 36 \pm 3$ arc s. These and earlier radius measurements[7,9] are plotted against the Julian Day (JD) number in Fig. 3. The large error bars assigned to measurements from ref. 9 reflect the fact that the radii were obtained from profiles which were computed in circular annuli centred on the nucleus instead of from cuts perpendicular to the orbital plane (inclination to the ecliptic ≈ 1.7°) and hence may contain the effects of radiation pressure. It is clear from Fig. 3 that the coma size is not symmetric with respect to perihelion (represented by a vertical dashed line) as would be expected for a normal coma[10]. Instead, a least squares fit to the data in Fig. 3 (excluding the lower limit at JD = 2,446,737.6) gives the constant coma expansion velocity $v = 1.1 \pm 0.2$ m s^{-1}. The fit is shown as the solid line in Fig. 3. There is good agreement with the previous best fit[7], $v = 0.9 \pm 0.2$ m s^{-1}, shown as a dashed line in Fig. 3. The inferred time of coma formation (the time at which the coma radius was zero) is $JD_0 = 2{,}443{,}934 \pm 900$ days ($R \approx 10$ AU), also in agreement with previous determinations[7,8].

The surface brightness of the coma of comet Bowell is <1% of the surface brightness of the night sky in the R filter (see Fig. 2), making accurate photometry extremely difficult. Our best estimate of the magnitude within an aperture of radius 5 arc s is $m_R(5'') = 21.7 \pm 1.0$ mag at $R = 13.6$ AU, where the large uncertainty is due to sky subtraction error and to variable extinction. At $R = 11.0$ AU the magnitude within an aperture of radius 5 arc s is $m_R\ (5.0'') = 20.0 \pm 0.2$. As a matter of interest, a crude estimate of the total brightness of the coma can be computed. We find $m_R \approx 17.9$ at $R = 11.0$ AU and $m_R \approx 20.5$ at $R = 13.6$ AU; even at 13.6 AU the comet is not particularly faint, only its diffuseness makes it hard to detect. In previous observations, the grain cross-section in a diaphragm of 5 arc s radius remained

Table 1 Observational parameters

JD (−2,440,000)	UT‡ (mid)	Exp§ (s)	Tel‖ (m)	Filter	χ airmass	α (1950)	δ (1950)	r (AU)¶	Δ (AU)#	Phase (deg)
6,737.6373	3:17:41	900	2.1	R	1.32	00:17:57.0*	00:0607	13.562	12.745	2.41
6,737.6734	4:09:42	900	2.1	R	1.23	00:17:56.0	00:06:07	13.562	12.745	2.41
6,737.7373	5:41:41	900	2.1	R	1.20	00:17:56.4	00:05:58	13.562	12.745	2.41
6,737.7726	6:32:35	900	2.1	R	1.26	00:17:55.5	00:05:55	13.462	12.745	2.41
6,329.9444	10:40:00	900	4	R	1.84	00:01:32.6†	−01:38:46	11.006	10.003	0.20

* Positions as measured at the telescope by offsetting from nearby SAO stars. The positions are accurate to approximately ±5 arc s.
† Positions accurate to approximately ±30 arc s.
‡ UT midtime of integration; § exposure duration in seconds; ‖ telescope diameter in m; ¶ heliocentric distance in AU; # geocentric distance.

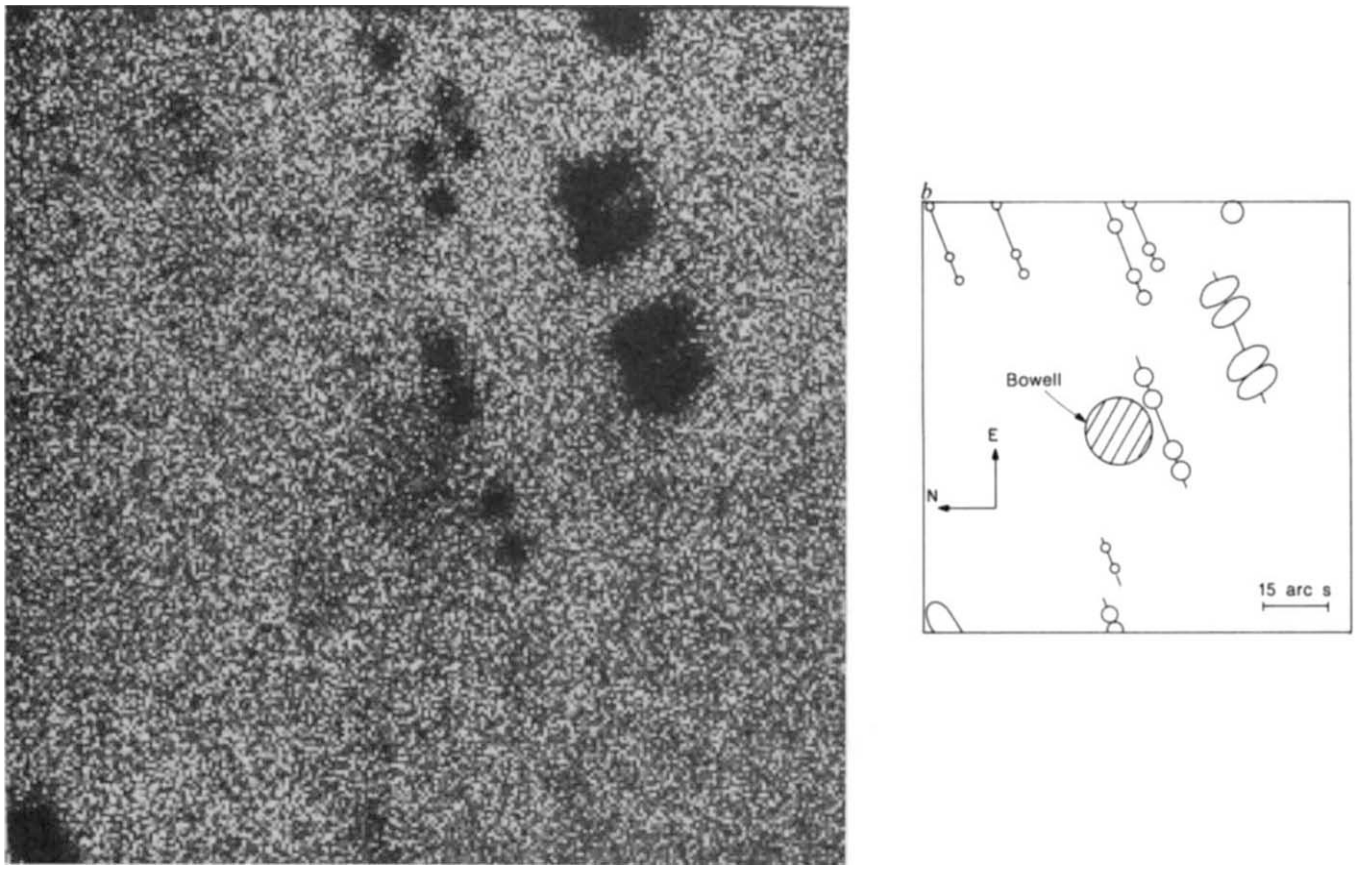

Fig. 1 *a*, CCD image of comet Bowell at $R = 13.6$ AU, taken 3 November 1986 UT. Four 900-s images were shifted according to the motion of the comet and a median filtered cubic spline function was fitted to the sky background near the comet and subtracted to produce this 1 h effective exposure. North is to the left and East to the top. The comet appears diffuse, with a total integrated magnitude within a diaphragm of 15 arc s radius of $m_R = 20.5 \pm 1.0$. *b*, Line diagram of Fig. 1*a* showing the location of the brighter field stars and galaxies with respect to the comet. The circle indicates the position but not the size of comet Bowell. A scale bar is shown for reference.

constant[7] at $C = (1.6 \pm 0.3) \times 10^9$ m^2 (where $C = 2.24 \times 10^{22} R^2 \Delta \pi 10^{0.4(m_{R(sun)} - m_{R(5'')})}/p$; and $p \approx 0.06$ (ref. 11) is the geometric albedo of the grains). The new photometry shows that the total cross-section has decreased by about an order of magnitude to $C = (1.8 \pm 0.3) \times 10^8$ m^2 at $R = 11.0$ AU and $C = 7 \times 10^7$ m^2 (within a factor of 2) at $R = 13.6$ AU. The quoted errors reflect not only the statistical uncertainty, but also the uncertainty in assuming a brightness profile which falls off as the inverse of the projected distance from the nucleus. Thus, the photometry suggests that the coma production is declining, and that the decline began at about the same critical heliocentric distance at which the activity began ($R \approx 10$ AU).

Numerous hypotheses have been put forward to explain the existence of cometary coma at large R, including (1) sublimation from small amounts of 'super-volatiles' such as CO_2 or C_2H_4 at large R (ref. 12); (2) gravitational perturbations by the sun on a dormant coma which is a remnant of the comet's formation[8], (3) electrostatic snap-off[7]; or (4) chemical instabilities[13] and phase transitions in the ice at low tempertures[14,15]. Of all these processes, the one which provides the most natural explanation for the appearance of a coma near $R = 10$–11 AU is the sublimation of material more volatile than H_2O. In particular, we are intrigued that near $R = 10$ AU, the momentum carried by sublimating CO_2 would just be sufficient to drag submillimetre particles into the coma from a nucleus of a few km radius.

The existence of CO_2 has been inferred in other comets. Comet Schwassmann–Wachmann 1 orbits the sun between 5–7 AU and has dramatic outbursts in which CO^+ has been detected[16]. It has been suggested that the sublimation of CO_2 or CO which is suddenly exposed to the surface is directly related the comet's activity[17]. In addition, CO_2^+ is frequently observed in cometary plasma tails. Recent observations of sudden increases in the column density of CO_2^+ ions in the tail of comet Halley suggest that CO_2 probably plays a role in the outbursts[18]. The birth and probable death of the coma of 1982 *I* near $R = 10$ AU, the

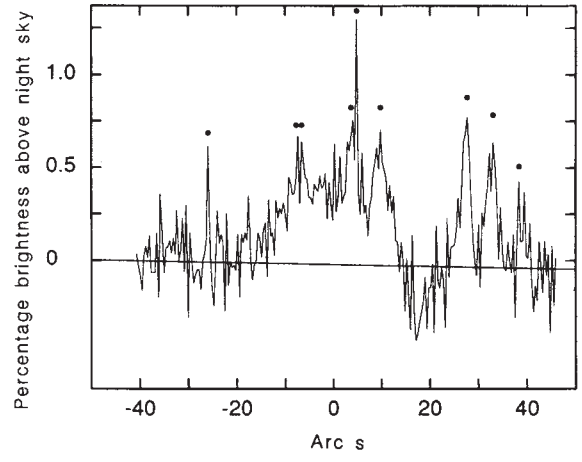

Fig. 2 Surface brightness profile E–W through comet Bowell at $R = 13.6$ AU. The profile is the mean surface brightness within a band of width 7.6 arc s centred on the comet. The level of the sky background is shown by a straight line. Several stars contaminate the profile; these are indicated by dots.

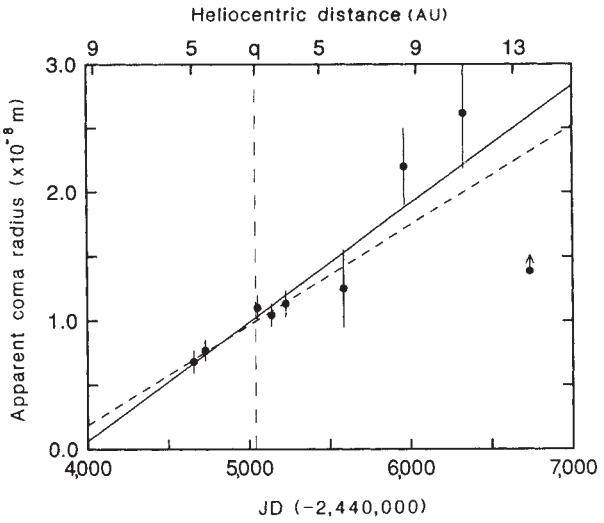

Fig. 3 Plot of the coma radius versus JD and heliocentric distance. Perihelion (at $q = 3.364$ AU) is marked with a vertical line. The least squares fit to the radius before 1984 is shown as the dashed line, the fit including the new data is shown as the solid line. The velocity of expansion is $v = 1.1 \pm 0.2$ m s^{-1}. The data point at JD = 2,446,737.6 represents a lower limit and is not included in the fit.

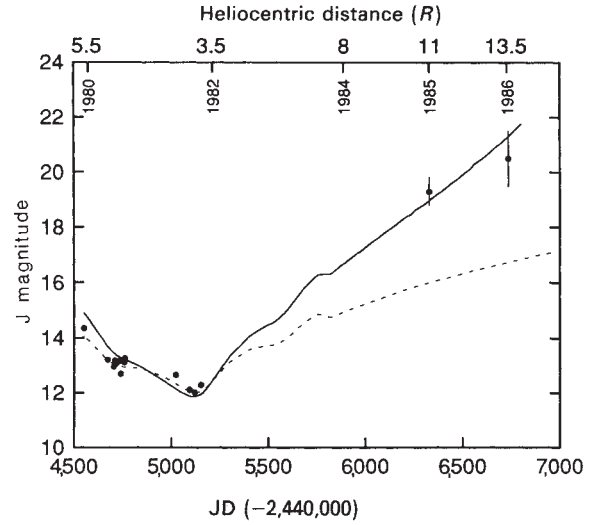

Fig. 4 J magnitudes with a 5 arc s radius diaphragm are plotted versus JD. The heliocentric distances and dates are marked at the top of the graph. The CO_2 sublimation model described in the text (solid line) is compared to the 'constant cross-section' model (dashed line).

existence of submillimetre grains in the coma and the ability of CO_2 sublimation to drag large grains from the coma at this distance all encourage a closer look at the CO_2 sublimation hypothesis.

To evaluate the feasibility of CO_2 sublimation for comet Bowell, we compare all of the available broadband photometry corrected to a 5 arc s radius diaphragm (the present photometry and that summarized in ref. 7) to a simple CO_2 sublimation model. The CCD R magnitudes (this paper) have been converted to the J bandpass (used in ref. 7) assuming $(R-J)_{sun} = 0.57$ (ref. 19). The model assumes equilibrium sublimation from a nucleus of negligible conductivity and is analogous to the model successfully applied to comet Halley (see ref. 3 for a complete description). Unfortunately, in the case of comet Bowell, relatively few of the input parameters are well known. What is known is an upper limit to the product of the 0.65 μm geometric albedo and cross-section of the nucleus[7], $C_n \leq 6 \times 10^6$ m^2; in addition, the analysis of the tail morphology provides a good estimate of the mean particle size[8]. Observations[7,11] also indicate that the albedo of the grains is low (we adopt $p \approx 0.06$). Figure 4 presents a comparison of the CO_2 model with the J magnitude in a 5 arc s radius diaphragm. It is interesting that the sublimating CO_2 model is able to fit the broadband photometry quite well. Also shown in Fig. 4 is a 'constant cross-section' model which shows the brightness variation that an extended source would have within a fixed diaphragm as the geometric factors changed (dashed line). This model fits the photometry well near perihelion, but is inadequate at larger distances.

A strict analogy with Halley would suggest that CO and not CO_2 should be the dominant volatile since the abundance of CO relative to H_2O is ~20% in Halley[20], whereas the abundance of CO_2 relative to H_2O is only ~3.5%[21]. Models for the much more volatile CO are compatible with the comet Bowell data only for very high-grain/nucleus albedos; however, high grain albedos are inconsistent with measured values[7,11].

The CO_2 sublimation model predicts that the terminal velocity of 300-μm grains in the outflowing gas should be of the order of 20 m s^{-1} at perihelion ($R \approx 3.36$ AU), decreasing as R increases. But the observed coma expansion velocity is $v \approx 1$ m s^{-1}, near the expected escape speed from the nucleus. It is difficult to reconcile the slow coma expansion with the expected 20 m s^{-1} terminal speed of the grains. One possible solution to this dilemma could be offered if the mass of dust ejected into the coma at high speed near perihelion were negligible compared to the total mass of dust present in the coma. The mass of dust in the observing diaphragm is equal to the integral of the mass loss rate over the time it takes the grains to cross the diaphragm. Therefore, if the comet experiences high ejection velocities and high mass loss for a relatively short time, it is possible that the total amount of material ejected at high velocity would represent only a small fraction of the total mass of dust in the coma and would hence be undetected. Unfortunately, our calculations indicate that the high terminal velocity is sustained for a period of time long enough that the high-velocity dust grains should have been readily detectable. Although the CO_2 model has difficulty explaining the observed low velocity of the grains, near perihelion the initiation of the coma near $R = 10$–11 AU and the apparent turn off at the same distance most strongly suggest sublimation of a material with the volatility of CO_2.

For grains moving at 1 m s^{-1}, the diaphragm crossing time is of the order of 1 yr. The comet has now been observed for more than 6 yr, significantly longer than the diaphragm-crossing time. The long diaphragm-crossing time effectively provides a long time constant for photometric changes. The nearly constant coma cross-section at $R \leq 10$ AU suggests that the mechanism producing the coma has been continuous and was not a single impulsive ejection at large R. The suggestion of an ice phase transition[15] thus seems unlikely on the basis that the coma was active both before and after perihelion whereas a phase transition would occur on the inbound journey as the comet first began to heat and would not naturally produce continued activity at the same distance post-perihelion.

The most distant recorded comet before Bowell, comet Stearns (1927 IV) at $R = 11.5$ AU (ref. 22), was also active at very large distances from the sun. Analysing photographic observations[22–24] from 1927–32, we find that comet Stearns was in some respects similar to comet Bowell (K.J.M., in preparation). Each comet had an extensive coma to $R \approx 10$–11 AU and both showed peculiar narrow tails. It will be crucial to obtain observations of comets which are active at very large heliocentric distances, of the type represented by comets Bowell and Stearns, to understand the source of the activity and to compare them with the short-period comets.

We are both Visiting Astronomers at the Kitt Peak National Observatory. We thank the efficient Kitt Peak staff for their excellent support, in particular we thank our telescope operator,

George Will. This work was supported in part by the NSF and NASA.

Received 28 January; accepted 30 April 1987.

1. Bowell, E. *IAU Circ.* No. 3465 (1980).
2. Everhart, E. & Marsden, B. G. *Astr. J.* **93**, 753-754 (1987).
3. Meech, K. J., Jewitt, D. & Ricker, G. R. *Icarus* **66**, 561-574 (1986).
4. Campins, H., Rieke, G. H. & Lebofsky, M. J. *Nature* **301**, 405-406 (1983).
5. A'Hearn, M. F., Dwek, E. & Tokunaga, A. T. *Astrophys. J.* **282**, 803-806 (1984).
6. Jewitt, D. C., Soifer, B. T., Neugebauer, G., Matthews, K. & Danielson, G. E. *Astr. J.* **87**, 1854-1866 (1982).
7. Jewitt, D. *Icarus* **60**, 373-385 (1984).
8. Sekanina, Z. *Astr. J.* **87**, 161-169 (1982).
9. Baum, W. A., Kreidl, T. J. & Schleicher, D. G. *Bull. Am. astr. Soc.* **18**, 794 (1986).
10. Mendis, D. A. & Ip, W.-H. *Astrophys. Space Sci.* **39**, 335-385 (1976).
11. Hanner, M. S., Veeder, G. J. & Matson, D. L. *Bull. Am. astr. Soc.* **3**, 705-706 (1981).
12. Mukai, T. *Astr. Astrophys.* **164**, 397-407 (1986).
13. Donn, B. & Urey, H. C. *Astrophys. J.* **123**, 339-342 (1956).
14. Smoluchowski, R. *Astrophys. J.* **244**, L31-L34 (1981).
15. Hanner, M. S. & Campins, H. *Icarus* **67**, 51-62 (1986).
16. Cochran, A. L., Barker, E. S. & Cochran, W. D. *Astr. J.* **85**, 474-477 (1980).
17. Cowan, J. J. & A'Hearn, M. F. *Icarus* **50**, 53-62 (1982).
18. Feldman, P. D. *et al. Nature* **324**, 433-436 (1986).
19. Johnson, H. L. in *A. Rev. Astr. Astrophys.* Vol. 4 (eds Goldberg, L., Layzer, D. & Phillips, J. G.) 193-205 (Annual Reviews Inc., California, 1966).
20. Woods, T. N., Feldman, P. D., Dymond, K. F. & Sahnow, D. J. *Nature* **324**, 436-438 (1986).
21. Krankowsky, D. *et al. Nature* **321**, 326-329 (1986).
22. Van Biesbroeck, G. *Astr. J.* **42**, 25-32 (1932).
23. Burton, H. E. *Astr. J.* **38**, 35-36 (1927).
24. Van Biesbroeck, G. *Astr. J.* **40**, 51-60 (1930).

Optical efficiencies of lightning in planetary atmospheres

W. J. Borucki & C. P. McKay

NASA Ames Research Center, Moffett Field, California 94035, USA

Spacecraft observations show that the presence of lightning activity is not confined to the terrestrial atmosphere, but is also found in the atmospheres of Venus[1], Jupiter[2] and Saturn[3]. Lightning activity may also occur in Titan's thick atmosphere. Calculations[4-6] show that lightning produces a significant fraction of the nitric oxide that reacts with the ozone and chlorine compounds in the terrestrial stratosphere. In the atmosphere of the primordial Earth, lightning could have been the major source of many of the molecules required for the formation of life[7]. To determine the effects of lightning activity in the atmospheres of other planets from spacecraft images requires a knowledge of the optical properties of the lightning discharge. Here we report the first simulations of lightning in planetary atmospheres by laser-induced plasmas. These simulations show that the fraction of the energy in lightning discharge channels that is radiated in the visible spectrum is similar for Earth, Venus and Titan, but quite different for Jupiter. One implication of our results is that the amount of trace gases produced by lightning in the jovian atmosphere must be larger than previously estimated.

It is expected that the trace-gas production rate by lightning will be proportional to the rate of energy dissipated by lightning activity. The energy dissipation rate can be estimated from the average optical energy dissipated per flash and the global flash rate if the optical efficiency is known. The optical energy dissipated per flash and the global flash rate are obtained from calibrated images taken by spacecraft. The optical efficiency is defined to be the ratio of the optical energy to the total energy deposited in the discharge column. Thus the determination of the optical efficiency is critical to the estimation of the trace-gas production rate by lightning.

Because of experimental difficulties, only estimates of the optical efficiency of terrestrial lightning have been reported previously. Connor[8] used a spectrograph with calibrated film and electric field data to obtain an estimate of 7×10^{-3} for the optical efficiency of terrestrial lightning. The uncertainty[4] in his estimate is at least a factor of four. To estimate more accurately the total energy dissipated in the discharge and the optical energy radiated by the discharge column, Krider *et al.*[9] used a silicon diode photometer to observe a 4-m spark in air. The electrical energy dissipated was determined in two ways: (1) integrating the product of the current and voltage with time; and (2) subtracting the energy stored in the impulse generator before and after the discharge. The agreement between the two measurements of the energy dissipation was within 40%. They conducted time-resolved spectroscopic studies of both the spark and lightning and found that both sources had similar spectra and should have similar optical efficiencies. They obtained an average optical efficiency of 3.8×10^{-3}.

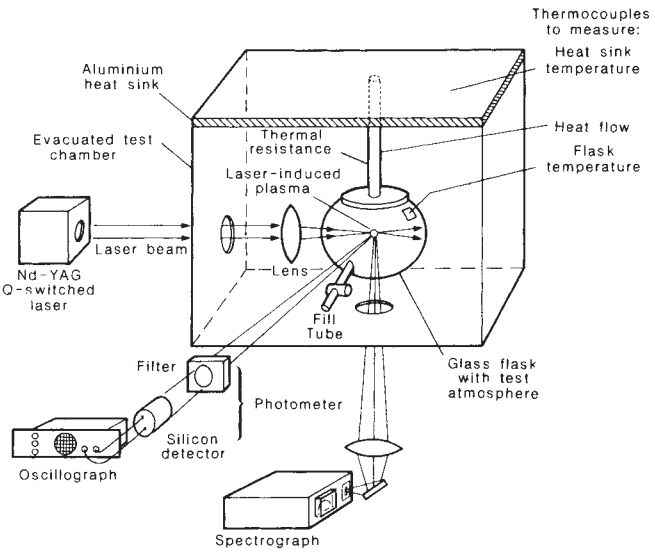

Fig. 1 Apparatus to measure optical efficiencies and spectral irradiance.

Recent measurements[10] in our laboratory have shown that the emission spectrum of terrestrial lightning can be simulated by laser-induced plasmas (LIP). Because such plasmas do not contact any electrodes, no contaminant spectra are present to interfere with the spectrum of the test gas and thus it is not necessary to use metre-long discharges to obtain adequate spectral purity of the optical radiation. A few cubic centimetres of gas are sufficient to produce the LIP and measure the optical efficiency. Hence, it is feasible to work with flammable gases like hydrogen and methane that are important components of planetary atmospheres.

Our measurements were made with a Q-switched Nd-YAG laser, a silicon diode detector, and a specially developed powermeter that measured the absorbed laser radiation.

Figure 1 is a sketch of the experimental apparatus. The flask with the test atmosphere is shown in the central portion of this figure. A 5-ns pulse of parallel light from the laser enters from the left, passes through a condensing lens to a focus at the centre of the flask. At the lens focus, the laser radiation causes gas breakdown and the formation of a high-temperature plasma. Any portion of the laser beam that is transmitted past the LIP exits through a window at the right-hand side of the test chamber. Laser radiation scattered from the plasma also passes out of the flask. Consequently, only power absorbed from the laser beam by the LIP is measured by the powermeter. The photometer measures the optical power as a function of time and records these data on an oscillograph. To exclude scattered laser radiation from the photometer, an optical filter that blocks the 1.1-μm laser radiation is used in front of the detector. The spectrograph verifies the purity of the test gases used.

To determine the total energy deposited by the laser in the LIP, the flask is placed in an evacuated chamber and the steady-state heat production in the flask is determined by measuring the temperature gradient at equilibrium in the aluminium rod